Aerodynamic Penalties of Heavy Rain on Landing Airplanes

P. Haines* and J. Luers†
University of Dayton Research Institute, Dayton, Ohio

The aerodynamic penalties due to very heavy rain on a landing aircraft is addressed in this paper. Based on severity and frequency of occurrence, torrential rainfall rates of 100, 500, and 2000 mm/h were investigated. Significant momentum loss was found to occur at moderate and higher torrential rainfall rates. The weight of a water film on transport category aircraft was found to be only a small fraction of landing weight. Roughness of an airfoil in rain is caused by drop cratering and waviness to a thin film on the airfoil and fuselage. Both sources of roughness were found to separately produce drag increases of from 5 to 10% for a 100-mm/h rain increasing to 15 to 25% for a 2000-mm/h rain. In addition, lift decreases of 10% for a 100-mm/h rain to more than 30% for a 2000-mm/h rain were estimated.

Exordium

IN recent years, wind shears associated with strong thunderstorm downdrafts have been implicated as the cause of several airplane accidents. The Eastern Flight 066 accident at Kennedy Airport[1] is a prime example. In the National Transportation Safety Board's reconstruction of the flight recorder data from the accident, extraordinarily large wind shears were estimated. The reconstruction considered no other external factors besides the wind. The performance degradation due to the torrential rain cell experienced by Eastern 066 was not taken into account. We feel it possible that the derived wind shears are too large because the effect of the very heavy downpour was ignored.

An extensive literature source revealed only one other investigation[2] which considered the effect of torrential rain on airplane performance. That investigation dealt with the case of an airplane encountering torrential rain at moderate altitude (about 5000 ft). It concluded that although torrential rain has a significant effect, its exposure time is insufficient to force the airplane to the ground. An airplane in landing configuration, however, does not have a wide margin of performance in which to overcome the aerodynamic penalties due to torrential rain. Thus in this paper and Ref. 21 we consider the importance of torrential rain to a landing airplane.

Rain can affect an airplane in at least four ways: 1) raindrops striking the airplane impart a downward and backward momentum; 2) a thin water film results from the rain that increases the airplane mass; 3) the water film can be roughened by drop impacts and surface stresses producing aerodynamic lift and drag penalties; 4) depending on airplane orientation, raindrops strike the airplane unevenly, thus imparting a pitching moment. In this article, we used mathematical modeling techniques augmented by experimental results found in the literature to assess the first three penalties. While weight and momentum penalties are relatively minor, those due to roughening of an airfoil by torrential rain can be very significant.

A roughened airfoil has long been recognized as a safety hazard for takeoff owing to the lift and drag penalties it produces. Even small roughness elements produced by nocturnal frost accumulation on an airfoil are of serious concern. Federal air regulations require the removal of frost from the wings of all transport aircraft prior to takeoff. Insect-produced roughness on the leading edge of an airfoil has also been known to produce aerodynamic penalties. Brumby[3] relates such an incident that occurred during a series of stall training flights.

Numerous wind tunnel tests have been conducted on an airfoil using artificially roughened surfaces such as sandpaper or ballotini.[2-5] These tests have measured both lift and drag penalties associated with roughness heights of only a fraction of a millimeter. The extension of these fixed roughness element tests to the case of fluid roughness is the basis of our investigation into the lift and drag penalties caused by intense rain.

The question is, "Can rain on an airfoil produce the same aerodynamic roughness effects that fixed roughness elements produce?" In attempting to answer this question we have theoretically modeled the rain roughness resulting from the craters formed when water drops impact with an airfoil at a landing velocity as well as the roughness produced by the waviness of a thin film of water that wets the airfoil. The modeling work has required certain assumptions whose validity could not be established at this time. Thus experimental validation of the results is necessary.

Nature of Heavy Rain

It is first necessary to establish the nature and frequency of torrential rain. Only short duration downpours associated with convective cells possess the intensity to seriously affect aircraft performance. We have chosen to categorize such rains by their rainfall rates in millimeters per hour.

Several authors have attempted to establish the frequency of occurrence of rainfall rates. Jones and Sims[4] performed an analysis of 1- and 5-min rainfall rates for many U.S. stations. The data used were only for a one-year period however, and the highest rate observed during that year was 238 mm/h at Miami, Fla. Hershfield[5] performed an analysis to obtain the expected mean maximum 5-min rainfall rate for stations throughout the U.S. He also estimated the maximum rainfall rates over 1-min periods to be about 50% higher than those over 5-min periods. These results give yearly mean maximum 1-min rainfalls of from 150 to 250 mm/h in the eastern United States. Information about rainfall rates for periods shorter than 1 min is unavailable. It is expected that very short period (from 20 to 30 s) rates are even greater than the maximum 1-min rates. The world record rainfall rate of 1828.8 mm/h or 73.8 in./h at Unionville, Md.[6] suggests an upper limit of 2000 mm/h.

For the purposes of this paper, the range of rainfall rates from 100 up to 2000 mm/h is termed torrential. Within the torrential classification a 2000-mm/h rain will be characterized as very heavy, a 1500-mm/h rain as heavy, a 1000-mm/h rain as severe, a 500-mm/h rain as moderate, and a 100-mm/h rain as light. Rain rates in excess of 500 mm/h are quite infrequent, but even though a 500-mm/h rain rate is an

Received July 1, 1981; revision received April 26, 1982.

*Research Meteorologist.
†Senior Research Scientist.

unlikely occurrence at a single station, the chances that it will occur at one or more stations in the eastern United States each year are considerably greater. A rainfall rate of 100 mm/h or greater is expected at least once a year in most of the eastern United States. Though the analysis is carried out over this entire range of rainfall rates, the rates of primary interest will be those less than 500 mm/h. Aircraft accidents are most likely associated with these rates.

To analyze the effect of heavy rain on aircraft performance, the size distribution of water droplets under different rainfall rates is required. The Marshall-Palmer[7] drop size distribution models the actual drop size distribution of rain reasonably well. Their results show that the size distribution can be approximated by the exponential function

$$\frac{dN(D)}{dD} = N_0 e^{-\psi D} \tag{1}$$

where $\psi = 41R^{-0.21}$ and $N(D)$ is the number of drops within diameter range dD, N_0 is an empirical constant (0.08), D is the drop diameter, and R is the rainfall rate in mm/h. The distributions described by Eq. (1) were originally derived from extratropical rains, but Merceret[8] found it valid for tropical showers as well.

The terminal velocity of raindrops of drop diameter D has been established by Markowitz[9]:

$$V(D) = 9.58\{1 - \exp[-(D/1.77)^{1.147}]\} \tag{2}$$

where $V(D)$ is the terminal velocity. A correction for terminal velocity aloft is

$$V(D) = V_0(D)(\rho_0/\rho_a)^{0.4} \tag{3}$$

where $V_0(D)$ is the terminal velocity for density ρ_0, ρ_0 is the density aloft, and ρ_a is the density at the surface. Equation (3) allows terminal velocity adjustment for aircraft operating at higher flight levels.

It is also necessary to know the percentage that each size droplet comprises of the total rain volume. The percentage can be calculated given the terminal velocity of each size droplet and the number of droplets in that size range. Following Markowitz,[9] the fraction of total rain volume due to raindrops of diameter D is

$$M(D)\,dD = N(D)(4/3)\pi(D/2)^3 V(D)\,dD \div \int_0^\infty N(D)(4/3)\pi(D/2)^3 V(D)\,dD \tag{4}$$

where $M(D)$ is the percent volume of total rain volume of drops of diameter D.

Impingement Efficiency

Obviously, not all drops in the path of an aircraft strike it. Some, especially smaller drops, are carried over or under the aircraft by the flow of air caused by the aircraft motion. A first step in calculating the aircraft momentum loss due to rain is calculating the ratio of the rain that strikes the aircraft to the total that would have struck the aircraft in the absence of the aircraft-induced airflow. This ratio is called collection or impingement efficiency.

We first calculated impingement efficiencies for a range of drop diameters from 0.5 up to 8 mm. By knowing the relative percentage of each drop size, it was possible to establish impingement efficiencies by rainfall rate by summing the product of impingement efficiency and relative volume percentage for all drop sizes.

A water drop trajectory program together with a potential flow model were used to calculate overall collection efficiencies of water drops by the airfoil of an airplane. The potential flow model calculated airflow about the airfoil. The airflow was used in calculating the paths of raindrops. The calculations were done in proximity to the aircraft for a range of drop size diameters. For momentum calculations, a summation of the products of collection efficiency times percentage contribution by drop diameter was made for each rainfall rate. Details can be seen in Haines and Luers.[10]

The overall collection efficiency for a given drop diameter is the ratio of drops that strike the airfoil to those that would have struck the airfoil had the airflow not affected the drop trajectories. This ratio can be expressed as $E = (Z_H - Z_L)/H$, where H is the projected height of the airfoil onto the initial drop position and Z_H and Z_L are the initial drop positions for, respectively, the highest and lowest drops to impact the airfoil (see Fig. 1a).

The overall collection efficiency by rainfall rate, C_E, is obtained by summing the product of drop size collection efficiency and percent volume contribution for all size drops. The summation was done for drop diameters from 0.5 to 8 mm in 0.5-mm increments.

$$C_E = \sum_{i=1}^{16} E_i M(D)_i$$

where E_i and $M(D)_i$ are, respectively, the overall drop collection efficiency and percent rain volume of the ith size drop. The overall collection efficiencies are greater than 95% for torrential rainfall rates. Similar results are anticipated for other airfoils and for the fuselage. Large angles of attack may decrease somewhat the overall collection efficiencies.

Determining where a raindrop has impacted the wing is crucial to calculating the local collection efficiency at various segments of the airfoil as well as calculating other impact parameters. Local collection efficiency is required in assessing the water film that may develop on the wing owing to heavy rain in addition to assessing the roughness that may develop in the film. The local collection efficiency, β, is the vertical distance between drop trajectories, dz, divided by the distance along the wing between successive impacts, ds (see Fig. 1b). Using the droplet trajectory program, local collection ef-

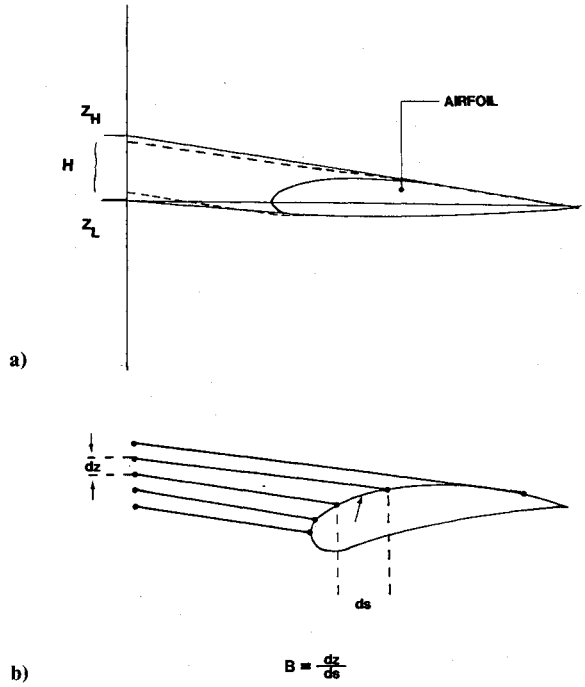

Fig. 1 a) Tangential drop trajectories for potential airflow about an airfoil. Drop trajectories begin well ahead of the airfoil to ensure that initially their paths are unaffected by the airflow. b) Calculation of local collection efficiency.

ficiencies were calculated for each droplet diameter at various stations around the airfoil. Local collection efficiencies by rainfall rate were then established at each station by weighting the percentage volume contribution of each droplet diameter by the local collection efficiency for that diameter and summing by drop diameter.

Momentum of Raindrops

Raindrops striking an airplane lose momentum to the airplane, thus changing the velocity of the airplane. The vertical component of the raindrop velocity imparts downward momentum to the airplane, which tends to make it sink. The raindrops striking head-on slow the airplane because momentum is lost in accelerating the water droplets to the airplane velocity. The amount of momentum imparted to an airplane by striking a raindrop depends on the reflection angle of the raindrops. A raindrop striking an airplane surface at an acute reflection angle imparts less momentum than if it strikes at a larger reflection angle. To estimate the impacted momentum for a large airplane such as a Boeing 747, the following assumptions were made:

1) All rain impinging on the airplane accelerates to the velocity of the airplane (inelastic collision).

2) The aircraft is in straight and horizontal flight at 0-deg angle of attack.

3) The flaps are not deployed.

4) The airplane goes from the no-rain to rain situation instantaneously.

The assertion that the impacts are inelastic is supported by Lucey's[11] work on the crush of a point detonating element (PDE). The PDE was mounted on a rocket sled and passed through a heavy rainfield. The measured crush of the element was related to work energy and was compared to the work that would have been done by both elastic and inelastic collisions. The comparison showed the measured crush could be best explained by inelastic collisions.

The calculation of rain-induced momentum penalties does not consider a landing wing configuration using flaps; this would present a larger impact cross section than does a wing in horizontal flight. Likewise, a nonhorizontal aircraft attitude should generally present a larger impact cross section. A greater momentum penalty would result in both cases.

The above assumptions used in calculating momentum penalties may overestimate the effect in some areas and underestimate it in other areas. Nonetheless, we believe they exhibit sufficient realism for an initial aerodynamic assessment. More details on momentum penalties can be found in Haines and Luers.[10]

Evaluation of the total force exerted on a 747 aircraft and the x and z components of this force for horizontal flight at 65 m/s (~125 knots) and 0-deg angle of attack are shown in Table 1 by rainfall rate. The additional force needed to balance the momentum penalty can be compared with the thrust produced by the airplane engines. For a 747 airplane the maximum engine thrust is on the order of 800,000 N (180,000 lb). Thus at a rainfall rate of 100 mm/h only 0.4% of maximum thrust is needed to counteract the rain momentum while at a 2000-mm/h rate 9% of maximum thrust is required.

If no additional thrust were applied and the other forces on the airplane remained constant then the rain momentum would extract speed from the airplane. The resulting deceleration equals the momentum force divided by the mass of the airplane. The deceleration for a 180,000-kg airplane varies from 0.04 knots/s at 100 mm/h to 0.2 knots/s at 500 mm/h to 0.75 knots/s at 2000 mm/h. If the airplane were in the torrential rain environment for a 20-s period, the approximate resulting loss of airspeed would be 0.8 knots for the 100-mm/h rate, 4 knots for the 500-mm/h rate, and 15 knots for the 2000-mm/h rate. These calculations of airspeed loss could be an underestimation for a landing configuration with high lift devices extended (which increases the water catch rate), or for a landing at a higher approach velocity (larger momentum loss), or when applied to an airplane executing a go-around maneuver (increased water catch rate). Nevertheless it appears that significant momentum penalties result for transport class airplanes only for rainfall rates of 500 mm/h or greater. For rates less than 500 mm/h, typical of most accident scenarios, the momentum penalty may be a contributing factor but of itself would not be expected to present severe problems. These momentum penalties are further analyzed in an adjoining article, using a landing simulation program to assess their effect on airplane performance.

Table 1 Force exerted on aircraft owing to momentum of drops

Rain rate, mm/h	ρ_{lw}, g/m^3	W_0, m/s	F, N	F_x, N	F_z, N
100	3.23	8.42	3.60×10^3	3.57×10^3	4.57×10^2
200	6.23	8.96	7.13×10^3	7.06×10^3	9.67×10^2
500	15.31	9.14	1.82×10^4	1.80×10^4	2.62×10^3
1000	30.18	9.30	3.58×10^4	3.54×10^4	5.17×10^3
2000	59.74	9.45	7.09×10^4	7.01×10^4	1.02×10^4

B-747 Aircraft

$V_{AC}=65$ m/s $A_T=1131$ m^2 $A_F=119$ m^2 $C_E\simeq1.0$

Water Film

In torrential rain, a water film forms on the upper surfaces of the wings, fuselage, and tail. The film may profoundly affect aircraft performance not only by increasing aircraft mass, but also by increasing total aircraft drag and by decreasing lift. For the purposes of assessing these aerodynamic penalties, it is necessary to calculate the film's mean thickness. In order to arrive at the film thickness, a number of assumptions were made.

Because the film is relatively thin and thus moves considerably slower than the airflow above it, the water film is assumed to be laminar. Its primary motivation is due to the airflow. At the interface viscous stress is matched between air and water. The resulting film is a balance between water runback and rain water reception. We assume the rain water reception is not affected by droplets shedding from the drop impact crowns. The shed droplets are probably returned to the film by boundary-layer entrainment.

The local rate of mass reception is required for calculating the film thickness. The reception rate is dependent on the liquid water content of the air, ρ_{lw}, the freestream airspeed, $\vec{V}_{\text{free}}$, and the local collection efficiency, β. For a given location the reception rate per unit area is given by

$$\dot{M}=\rho_{lw}\beta\vec{V}_{\text{free}} \tag{5}$$

A numerical model for the water film was developed to calculate film thickness by airfoil location and rainfall rate. The model geometry calculates the film flow at a number of stations along the wing as shown in Fig. 2. At each station, the film thickness results from water remaining after the gains and losses due incoming rain and film flow are considered. After a time, an equilibrium thickness results at each station. A more complicated model that considers pressure gradient, gravity, and other effects is not warranted as a first look at heavy rain effects on airplanes. Refinements to the model may be desirable in the future however.

The mass balance at a station, i, may be expressed as

$$\frac{dm_i}{dt}=\frac{\rho_w}{A}\int_{\substack{z=0\\x=i\Delta x}}^{z=h} u\,dz-\frac{\rho_w}{A}\int_{\substack{z=0\\x=(i+1)\Delta x}}^{z=h} u\,dz+\frac{\partial m_i}{\partial t} \tag{6}$$

where the first and second terms represent respectively mass flux into the ith station ($x=i\Delta x$) of area A and out of the

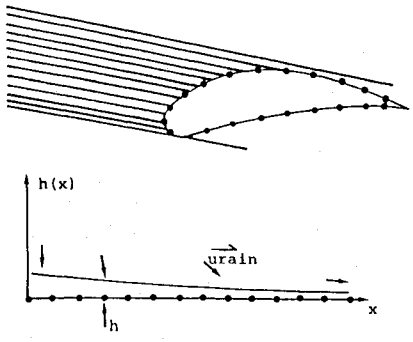

Fig. 2 Water film thickness model.

Table 2 Average film thickness for a symmetric airfoil and fuselage at 0-deg angle of attack, 10-m chord

Rainfall rate, mm/h	Calculated thickness airfoil, mm	Estimated thickness fuselage, mm
100	≤0.2	≤0.2
200	0.5 or less	0.2 or less
500	0.8	0.6
1000	1.0	0.9
2000	1.3	1.1

station ($x=(i+1)\Delta x$) due to film flow. Term 3 represents mass flux, into the ith station due to rain.

A new film thickness results from

$$h_i = \frac{(m_i + (\mathrm{d}m_i/\mathrm{d}t)\,\Delta t)}{\rho_w A} \tag{7}$$

The procedure is repeated for each station from first to last and continues until an equilibrium h_i has been attained.

A linear velocity profile is assumed between specified velocities at the film's top and bottom. At the bottom, the film velocity is zero. At the top, the velocity is based on the viscous stress due to the airstream above the water film. Following Hartley and Murgatroyd,[12] the shear stress at the surface of the film is

$$\tau = C_F \rho V_a^2/2 \tag{8}$$

where C_F is the air friction coefficient, ρ is the air density, and V_a is the average air velocity over the wing. The velocity in the film at any height z is

$$u = \tau z/\mu \tag{9}$$

where μ is the water viscosity.

The resulting average film thicknesses for the top of the airfoil derived from the model by rainfall rate are summarized in Table 2. The calculations were made for a symmetric airfoil of chord length 10 m at 0-deg angle of attack and 65-m/s (126-knots) freestream airspeed.

The film thicknesses for the fuselage were estimated from calculations for an airfoil. Because of increased impact surface area on the fuselage in relation to its projected area, the droplet impact density on the fuselage is approximately two-thirds that on the airfoil. Thus the mass impact rate per unit area on the fuselage is only two-thirds that of the airfoil. As a first-order approximation, the fuselage film thickness at a given rainfall rate was estimated as the airfoil film thickness that corresponds to two-thirds the given rainfall rate.

Weight Penalty

The weight penalty is due to the weight of the water film on the surface of the airplane. Film thickness was not calculated for the lower surface, below the stagnation point. If a film exists there, it would be expected to be thinner because of a decreased water impact rate. Even assuming the film on the underside were equally thick, it would only double the weight. For a 747 airplane whose landing weight is on the order of 180,000 kg, the maximum weight penalties cannot be much larger than 1% landing weight. A 1% added weight has a negligible effect on airplane landings.

Airfoil Roughness

An airfoil or fuselage in heavy rain may be roughened in at least three ways: 1) drops impacting a water film disturb its surface, 2) waves develop in a water film clinging to the wings and fuselage, 3) in the absence of a liquid film, globules dot the wing surface and are blown back by wind stress.

This study has analyzed two of the roughness sources. They are the roughening of a water film on an airfoil's top surface due to drop impacts and the roughness due to waves in the water film. Future modeling can consider the blow back of liquid water globules.

Roughness Due to Impact

We have investigated the impact of a raindrop on a thin film based on the work of Macklin and Metaxas,[13] who studied the craters formed when a water drop impacts a thin water film. Unfortunately their study was conducted at drop velocities considerably slower than those impacting an airplane wing. Thus extrapolation of their results to higher velocities was required.

The raindrop splash model assumes that a drop hitting a thin film forms a cylindrical crater. All the water originally residing within the crater is assumed to go into the crater crown. Virtually no wave swell results from the impact. An energy balance equation relating the nondimensional crown height to crown radius in terms of the inertial, gravitational (Froude number), and surface tension (Weber number) energies is given by[13]

$$(H^*)_{\text{theor}} = \frac{1 + 6(W_b)^{-1} + 2(F_N)^{-1} - 3(W_b)^{-1} D^* R_c^*}{6(W_b)^{-1} R_c^*} \tag{10}$$

where $W_b = \rho_w R_d V_{\text{free}}^2/\sigma$ is the Weber number (ratio of inertial to surface tension force); $F_N = V_{\text{free}}^2/gR_d$ is the Froude number (ratio of inertial to gravitational force); $D^* = h/R_d$ is the dimensionless depth of liquid film; $H^* = H/R_d$ is the dimensionless crown height; $R_c^* = R_c/R_d$ is the dimensionless crown radius; $t^* = V_{\text{free}} t/R_d$ is the dimensionless time; R_d is the drop radius; σ is the surface tension; and h is the film thickness.

Equation (10) does not take into account viscous forces (which contribute less than 7%) and other influences not accounted for in this idealized model. In comparing this model with experimental data, Machlin and Metaxas found the model accounts for from 40 to 60% of the energy dissipation in thin film impacts. The unaccounted energy is thought to predominately consist of surface energy. The solution of Eq. (10) requires the use of an empirical relationship between dimensionless crown height H^* and crown radius R_c^*. Figure 3a shows the ratio of H^*/R_c^* for different Weber numbers. It was necessary to extrapolate the curve from Fig. 3a to much higher Weber numbers appropriate to drops impacting on an aircraft. An extrapolated ratio of 2.9 was used for Weber numbers of approximately 5×10^4. Although use of such a severely extrapolated value was undesirable, a sensitivity analysis using other ratios of H^*/R_c^* (Refs. 1 and 5) did not change the essential results of the analysis. Using the extrapolated ratio, H^* is theoretically obtained from the solution of Eq. (10). The theoretical crown height is then adjusted by Fig. 3b to account for the energy dissipated that is unexplained by the model.

The dimensionless time to reach maximum crown height is obtained from Fig. 3c as a function of experimental and

theoretical values of H^*. Figures 3a-3c each required severe extrapolation of the experimental data for the situation of rain impacting on an airplane.

The values derived for maximum crown height, radius, and time to reach maximum crown height are the basic parameters for deriving the aerodynamic roughness height due to drop impacts on an airfoil. Table 3 shows these parameters for a drop impact velocity typical of a transport aircraft landing.

Evaluating the roughness of a film due to drop impacts requires knowing two parameters. One parameter is the mean height of a drop impact crown throughout its life cycle from formation to dissipation. The other parameter is the mean separation distance between drop impacts. Both parameters can be calculated from the results in Table 3 along with local collection efficiencies, β.

The mean separation distance is derived from the rate of drop impacts and the time over which a drop impact persists. The rate of drop impacts of diameter D at a given location on the airfoil is the product of drops per unit volume times the freestream airspeed times the local collection efficiency. The time period δt over which a drop impact crater exists is conservatively approximated as twice the time required for a crater to reach maximum crown height, that is,

$$\delta t = t_c^* D / V_{\text{free}} \tag{11}$$

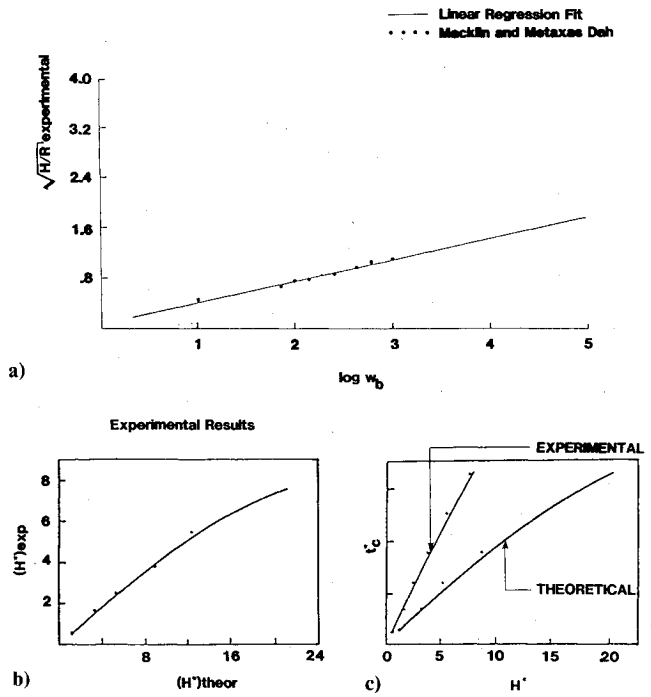

Fig. 3 a) Ratio of crown weight H to cavity radius at maximum crown height as a function of Weber number using Macklin and Metaxas (1976) data. b) Dimensionless crown height as a function of theoretical values from Eq. (10) (after Macklin and Metaxas, 1976). c) The dimensionless time to reach maximum crown height t_c^* as a function of the theoretical and experimental values of H^* for shallow liquid splashing (after Macklin and Metaxas, 1976).

The number of drop impact crowns of diameter D occurring at any given time is

$$N(D)\, V_{\text{free}}\, \delta t \beta = N(D)\, t_c^* \beta D \tag{12}$$

where $N(D)$ is the number of drops of diameter D per unit volume in free air. Using the Marshall-Palmer distribution to represent $N(D)$ and integrating the above over all D gives the total number of drop impact craters at a given time,

$$N = \int_{D=0}^{\infty} N_0 e^{-\psi D} t_c^* \beta D \mathrm{d}D = N_0 t_c^* \beta / \psi^2 \tag{13}$$

In integrating Eq. (13) both t_c^* and β are assumed constant as they are slowly varying functions of D.

The mean separation distance is given as the inverse square root of the number of drops involved in an impact at any instance of time per unit area. That is,

$$\bar{D} = 1/\sqrt{N} \tag{14}$$

For a drop of diameter D, the average drop impact crown height over its lifetime is conservatively approximated as one-half of its maximum crown height. That is,

$$k(D) = H_{\text{exp}}^* D/4 \tag{15}$$

The average height, $\bar{k}$, for a population of drop impact craters of varying diameters is the population weighted mean

$$\bar{k} = \frac{\int_{D=0}^{\infty} k(D) N(D) \mathrm{d}D}{\int_{D=0}^{\infty} N(D) \mathrm{d}D} \tag{16}$$

The evaluation of Eq. (16) again assumes t_c^* and β are constant and that $N(D)$ is represented by a Marshall-Palmer distribution. Thus

$$\bar{k} = H_{\text{exp}}^* D / 2\psi \tag{17}$$

where $\bar{k}$ is considered to be the height of the roughening elements produced by drop impacts.

The roughness height is estimated based on from Eqs. (14) and (15) by finding the equivalent sand roughness.[14] Also required was the ratio of the projected area of drop crowns in the freestream velocity direction, A_p, to the windward surface area, A_s, of the element as seen by the flow. This ratio is about 0.64 for cylindrical drop impact crowns. From Dirling, the sandgrain roughness correlation Λ is related to the spacing parameter, $\bar{D}/\bar{k}$, as

$$\Lambda = (\bar{D}/\bar{k})\,(A_p/A_s)^{-4/3} \tag{18}$$

Considering for simplicity, a rainfall rate to be characterized by droplets all of the same diameter (the volume mean diameter for that rainfall rate) and using the average local collection efficiency for the entire airfoil, values for $\bar{D}$ and $\bar{k}$ were calculated from Eq. (18) for a freestream velocity of 65 m/s and are given in Table 4.

Table 3 Drop impact velocity parameters typical of a transport aircraft landing

Drop radius, mm	$V = 65$ m/s					
	W_b	F_N	$H^*/R^*_{c_{\text{exp}}}$	H^*_{theor}	H^*_{exp}	t_c^*
0.5	2.98×10^4	8.61×10^5	2.79	113.94	13.2	41.55
1.0	5.79×10^4	4.31×10^5	2.98	169.48	14.6	43.40
2.0	1.158×10^5	2.15×10^5	3.25	250.35	15.9	45.00
4.0	2.312×10^5	1.08×10^5	3.53	368.71	16.8	46.00

Table 4 Average spacing between raindrop impacts and geometric height of impact crowns by rainfall rate

Rain rate, mm/h	$\bar{D}$, cm	Height $\bar{k}$, mm
100	20.16	4.8
200	17.43	5.6
500	14.38	6.7
1000	12.43	7.8
2000	10.74	9.0

Table 5 Sand grain roughnesses by rainfall rate

Rain rate, mm/h	k_s, mm
100	0.18
200	0.37
500	0.89
1000	1.83
2000	3.65

From Dirling the correlation equation for sandgrain roughness k_s with Λ is

$$k_s/\bar{k} = 0.0164\Lambda^{3.78} \qquad \Lambda \leq 4.93$$

$$= 139\Lambda^{-1.9} \qquad \Lambda \geq 4.93 \tag{19}$$

The average sand grain roughnesses by rainfall rate derived in Eq. (19) are given in Table 5.

To make estimates of the drag increase due to these values of sand grain roughness, results from Young[15] for fixed roughness elements with turbulent flow over a flat plate were utilized. The mean friction coefficient C_{F_S} for smooth wall flow is given by

$$C_{F_S} = 0.088/(\log Re - 1.5)^2 \tag{20}$$

In roughened flow the mean friction coefficient is

$$C_{F_R} = (1.89 + 1.62\log L/k_s)^{-2.5} \tag{21}$$

where L is the mean aerodynamic chord or fuselage length. For a 747 wing the Reynolds number in the landing configuration is $Re \simeq 3.23 \times 10^7$, while for the fuselage it is 2.74×10^8. Values of C_{F_S} and C_{F_R} for a 747 by rainfall rate are shown in Table 6.

An estimate of the influence of increased frictional drag on total drag for the 747 aircraft in the landing configuration can be approximated as follows. For a 747 aircraft with 30-deg flaps descending a glide slope at 2-deg angle of attack the basic drag coefficient including landing gear is approximately $C_{D_0} = 0.15$.[16] The basic drag coefficient can be decomposed into contributions from airfoil and fuselage friction coefficients as

$$C_{D_0} = 2C_F^{\text{air}} + C_F^{\text{fus}} A^{\text{fus}}/S + C_{D\,\text{etc}} \tag{22}$$

where A^{fus} is the total surface area of the fuselage, S is the wing area (upper surface), and $C_{D\,\text{etc}}$ are all other factors that contribute to C_{D_0}. The factor 2 in the first term on the right-hand side accounts for friction drag on both upper and lower wing surfaces. A representative value for the surface area ratio for a 747 aircraft is

$$A^{\text{fus}}/S \simeq 3.4$$

Table 6 Mean friction coefficient for smooth and roughened airfoil ($L = 8.3$ m) and fuselage ($L = 70$ m)

Rain rate, mm/h	C_{F_S} Airfoil	C_{F_R} Airfoil	C_{F_S} Fuselage	C_{F_R} Fuselage
100	0.0024	0.0036	0.0018	0.0025
200	0.0024	0.0042	0.0018	0.0028
500	0.0024	0.0051	0.0018	0.0033
1000	0.0024	0.0059	0.0018	0.0038
2000	0.0024	0.0069	0.0018	0.0043

Table 7 Increase in total drag due to increased wing and fuselage friction drag (747 aircraft landing configuration)

Rainfall rate	$\Delta C_D/C_{D_0}$, %
100	1.6
200	2.3
500	3.5
1000	4.6
2000	5.9

For an aircraft whose upper surfaces are roughened by rain, the change in C_{D_0} due to increased friction drag is

$$\Delta C_{D_0} = \underbrace{C_{F_R} - C_{F_S}}_{\text{Airfoil}} + \underbrace{(A/2S)(C_{F_R} - C_{F_S})}_{\text{Fuselage}} \tag{23}$$

Using the appropriate values from Table 6 in Eq. (23), the percent changes in C_{D_0} for a 747 aircraft in the landing configuration are shown in Table 7.

The increases in drag coefficient shown in Table 7 are significant. If both the upper and lower surfaces of fuselage and airfoil were roughened to the same extent, the values shown in Table 7 would increase by a factor of 2.

To establish the validity of applying Eqs. (20) and (21), which refer to flat plate turbulent flow conditions, to an airfoil with extended flaps, a comparison of theory to experimental wind tunnel measurements by Ljungstroem[17] was made. Ljungstroem measured both lift and drag increments on a two-dimensional wing section with and without high lift devices. The wing chord length was $\simeq 65$ cm. Figure 4a shows C_D and C_L curves for a clean wing and a roughened wing (95 and 100% coverage) with various sand grain roughness elements. Using Eqs. (20) and (21), the smooth and roughened friction coefficients for this case were calculated as $C_{F_S} = 0.0036$, $C_{F_R} = 0.0052$ ($k_s = 0.1$ mm), and $C_{F_R} = 0.0076$ ($k_s = 0.5$ mm). The values are shown in Fig. 4a after converting to drag coefficient. Note that Eq. (20) gives a good approximation to the smooth airfoil drag coefficient but Eq. (21) grossly underestimates the roughness penalty by a factor of 3 or more. Since the wind tunnel measurements include pressure drag as well as friction drag it is apparent that additional drag penalties result from roughness above those calculated by Eq. (21). Similar results were obtained from Ljungstroem measurements on a high lift airfoil with 25-deg slats and 20-deg flap. Figure 4b shows the measured C_D vs C_L at low angles of attack. The experimentally derived increase in C_D between a clean and fully roughened airfoil is approximately $\Delta C_D = 0.025$ for $k_s = 0.5$ mm and $\Delta C_D = 0.009$ for 0.1 mm roughness. Calculated differences in skin friction coefficient are $\Delta C_D = 0.0040$ for $k_s = 0.5$ mm and $\Delta C_D = 0.0017$ for $k_s = 0.1$ mm. For this wing configuration the skin friction calculation underestimates the roughness-induced drag increase by a factor of from 5 to 6. Thus in applying the increase in friction drag calculated by Eqs. (20)

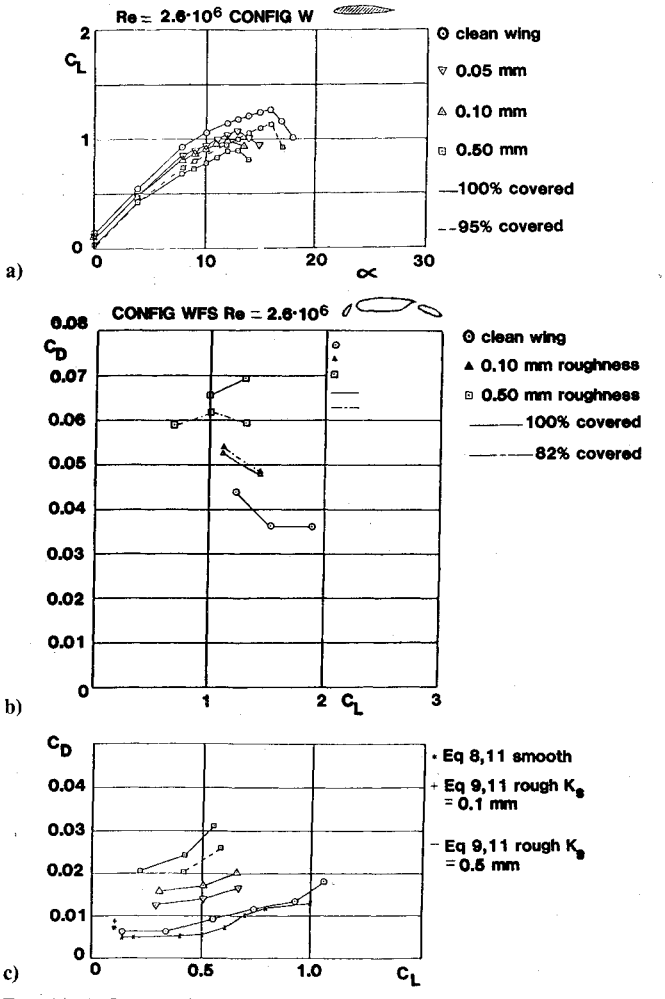

Fig. 4 a) C_L and C_D for configuration *W*, wing section, NACA 65 A-215 (after Ljungstroem, 1972). b) C_D vs C_L for configuration WFS, wing section with slat and trailing-edge flap (after Ljungstroem, 1972).

Table 8 Equivalent sand grain roughness of wavy water film

Rain rate, mm/h	Equivalent sand grain roughness k_s Airfoil, mm	Fuselage, mm
100	<0.3	<0.3
200	0.7	0.3
500	1.2	0.9
1000	1.5	1.4
2000	2.0	1.7

and (21) as the sole contributor to increased drag coefficient, underestimation by a factor of from 3 to 6 appears likely. Consequently the percentage drag penalties due to roughness shown in Table 7 should be increased by a compensating factor—perhaps on the order of 3.

Roughness Due to Film Waviness

Surface waves are observed on water film surfaces under wind stress.[18] They have been shown to have a comparable effect on airflow as sand-roughened walls. Wurz[19] conducted an experimental program to study the interference of a wavy liquid film with a turbulent gas boundary layer. Using a wind tunnel of 0.75 m in length, with airflow over a thin film and appropriate instrumentation, Wurz measured various interactions of the water film and its interface with the air boundary layer for a range of Mach numbers from subsonic to supersonic. Of interest to our application for rain roughness on an airfoil are the results at low subsonic Mach numbers. Tests conducted in the Mach number range 0.18-0.6 produced film thicknesses in the range 0.014-0.2 mm. The water flow rates associated with these film thicknesses are an order of magnitude less than that produced by an aircraft penetrating a 300-mm/h rainfall rate at landing speed. Thus the results of the Wurz experimental work, even though it covers sufficiently low Mach numbers, must be extrapolated to thicker films than occurred in the experimental tests. His results indicate an increase in friction coefficient as the film thickness increases. Wurz[20] also measured a ratio relationship between the mean water film thickness and equivalent sand grain roughness to be between 1.25 and 2.0 in the subsonic test range. Using a ratio of 1.5 as representative, an equivalent sand grain roughness was derived for the airfoil and fuselage film thicknesses associated with from 100- to 2000-mm/h rainfall rates. Table 8 shows these results.

Table 9 Increase in drag coefficient due to film waviness

Rainfall rate, mm/h	$\Delta C_D/C_{D_0}$, %
100	2.1
200	3.2
500	3.8
1000	4.2
2000	4.6

Again using Eq. (21), we estimated the increased skin friction coefficient. Using Eq. (23), increases in friction drag were converted to percent increase on drag coefficient for waves on the upper surface of the wing and fuselage. Table 9 shows these results.

Drag increases in the range of from 2 to 5% are derived for the various rainfall rates. This drag increase is based solely upon an increased friction coefficient derived from Eqs. (20-23). If allowance is made for the experimental measurements of Ljungstroem, then the drag penalties due to film waves would increase by a factor of from 2 to 6 over those of Table 9. Thus there is reason to suspect that Table 9 may seriously underestimate the actual drag penalties associated with the waviness of the water film.

In comparing the derived drag penalty due to film waviness (Table 9) with that derived for drop impact cratering (Table 7), it is seen that the impact cratering penalty is approximately of the same order of magnitude as that associated with film waviness. However, the experimental data upon which the waviness calculations were based require less severe data extrapolation and thereby more confidence is placed in these values. In combining the drag estimates due to waviness with those due to drop impact cratering and taking into account the possible underestimating of these penalties when compared to experimental measurements, a best overall estimate of total drag penalty for a transport aircraft in the landing configuration was made. We estimate this penalty for 100-2000-mm/h rainfall rates to be in the range of from 10% at the lower rainfall rates and up to 50% or more for the highest rates.

Reduction of Lift Due to Roughness

Distributed roughness on the upper surface of an airfoil also affects lift. Brumby[3] summarized the results of 23 experimental investigations concerning the effect of roughness on lift coefficient and stall angle. Included in Brumby's analysis was the data of Ljungstroem for airfoils with and without high lift devices. (See Figs. 20 and 21 of Ref. 3.) For a fully rough airfoil with "large" roughness elements Brumby found the lift coefficient to decrease at all angles of attack. For "medium" roughness a decrease in the lift coefficient primarily occurs at high angles of attack. The decrease in maximum lift coefficient ($C_L$max) is related to the ratio of roughness element height to wing chord. Decreases in C_L max

Table 10 Reduction in maximum lift coefficient and angle of attack at stall due to roughness

Rain rate, mm/h	$\Delta C_L/C_L$		$\Delta\alpha_{C_{L_{max}}}$	
	Drop impact cratering, %	Film waviness, %	Drop impact cratering, deg	Film waviness, deg
100	7	11	1-2	1-3
200	13	20	1-3	2-4
500	25	25	2-5	2-5
1000	29	28	3-5	3-5
2000	34	30	3-6	3-5

as high as 34% occur for "large" roughness elements. A decrease in stall angle also accompanies a decrease in $C_L$max. A stall angle decrease of from 3 to 5 deg is appropriate for a decrease in $C_L$max of from 25 to 30%, while a 1- to 3-deg decrease in stall angle is appropriate for lift losses of from 5 to 15%. An increase in stall speed also occurs. Stall speed increases of from 10 to 20 knots accompany a loss in maximum lift of from 10 to 30%. For a roughened airfoil the drag coefficient also increases dramatically at high angles of attack because of the premature onset of stall.

Using the results of Brumby, estimates were made of the reduction in maximum lift and increase in stall angle for a rain-roughened airfoil in a landing configuration.

Using the sand grain roughnesses associated with drop impact from Table 5 and those associated with film waviness from Table 8, the reduction in maximum lift coefficient and the decrease in angle of attack at stall were calculated for a 747 aircraft. These calculations were derived from Brumby's curve for an airfoil with high lift devices retracted, whose entire surface is roughened.

Brumby further states that leading-edge high lift devices even in the extended position do not recover degraded lift owing to large amounts of roughness.

Table 10 shows a significant reduction of maximum lift and stall angle for roughness associated with both drop impact cratering and film waviness. Though unvalidated assumptions were necessary in deriving these results, we believe they are sufficiently realistic to warrant a most serious consideration of the influence of heavy rain on aircraft aerodynamics. Even the magnitude of lift penalties and stall angle decreases due to film waviness alone—for which our assumptions are best justified—could provide serious aerodynamic problems for an aircraft executing a go-around in a heavy rain environment. It is also likely that because of the decrease in stall angle, an aircraft may actually stall before activation of a stall warning device based upon clean airfoil aerodynamics.

Summary and Conclusion

This research has assessed the effects torrential rain has on airplane weight, momentum, and aerodynamics performance. It is expected that several aircraft per year while in landing configuration will be exposed to rainfall rates on the order of 500 mm/h, while many more will experience rates in excess of 100 mm/h. The momentum loss to an airplane penetrating a 500-mm/h rainfall rate could be significant, though it alone would not be expected to cause an accident. It could however be a contributing factor that produces a decrease in the airspeed. The momentum loss may be most critical for an aircraft climbing through heavy rain while executing a missed approach with high lift devices extended. The increased rate of airspeed loss during the climb could put the aircraft in a low kinetic energy situation. The weight penalty resulting from a film of water present on the aircraft while penetrating a heavy rain was found to be negligible.

The effects of a rain-roughened airfoil on the drag and lift coefficient of an aircraft have also been assessed. The airfoil roughness arises from two sources: cratering of the raindrops upon impact with the airfoil and the waves produced on the thin water film from air stress. The roughness produced by each of these sources was analyzed independently. Previous experimental work was extrapolated to model the cratering of droplets impacting the airfoil at a velocity typical of the landing speed of an aircraft. The height of the crater and its residency time vs the rainfall rate were used to determine the average sand grain roughness of the upper surface of the airfoil at a given instance in time. Two techniques were then used to derive a drag penalty from the calculated sand grain roughness. The first technique determined the increase in the friction coefficient of the airfoil and fuselage based upon friction coefficient equations for turbulent flow over a flat plate. The increase in friction coefficient was then converted to an increase in the aircraft drag coefficient based upon the friction coefficient contribution to total drag for an aircraft in the landing configuration. The second technique directly related average sand grain roughness to changes in the drag coefficient of a two-dimensional airfoil based upon experimental measurements. The former produced drag penalties on the order of from 2 to 6% for rainfall rates between 100 mm/h and the world-record rate of 2000 mm/h. The second technique, based upon experimental data, indicated drag coefficient penalties three to six times as large as those attributable to the skin friction component. A similar procedure was used to estimate aircraft drag coefficient penalties resulting from the waviness of the film. The derived friction coefficient influence was found to be on the order of from 2 to 5%, while experimental two-dimensional airfoil measurements of drag coefficient penalty suggest they are at least three times as large. Based upon the above analysis and taking into account the uncertainties and assumptions that were required throughout the modeling, our best overall estimate of increase in the drag coefficient of an aircraft due to drop cratering and wave-induced roughness is on the order of from 5 to 10% at rainfall rates of 100 mm/h increasing to 30-50% at a rainfall rate of 2000 mm/h.

The decrease in maximum lift and increase in stall speed due to induced roughness on an airfoil was also assessed. The roughness associated with drop impact cratering produced losses in maximum lift of 37% at 100-mm/h rainfall to more than 30% at higher rates. Film waviness produced losses in maximum lift from 11 to 30% depending upon rainfall rate. Decreases in stall angle of from 1 to 6 deg and a corresponding increase in stall speed also result from these penalties to maximum lift.

These lift and drag penalties are of a magnitude sufficient to produce serious aerodynamic penalties on an aircraft when in a landing configuration in a thunderstorm. Thus we believe that aircraft penetrating heavy rain in a landing configuration may experience serious penalties that could potentially lead to an accident. Experimental validation of our results, however, is lacking, and must be pursued.

Acknowledgments

This research was supported by the Ground Flight Safety and Optical System Sections of NASA Wallops Flight Center through the General Aviation Office and Air Transport Office of the Office of Aeronautics and Space Technology (OAST), NASA Headquarters. The authors are indebted to Bob Carr, Raymond Rose, Roger Windblade, and Dick Tobiason of their respective NASA offices for support of this research. Special recognition is extended to Lloyd Parker and Ed Melson of NASA Wallops Flight Center, and Mark

Dietenberger and Charles MacArthur of UDRI, for their guidance and critique of this research program.

References

[1] National Transportation Safety Board, "Aircraft Accident Report," NTSB-AAR-76-8, Washington, D.C., 1975, pp. 47.

[2] Rhode, R.V., "Some Effects of Rainfall on Flight of Airplanes and on Instrument Indications," NACA Rept. No. 803, 1941.

[3] Brumby, R.E., "Wing Surface Roughness Cause and Effect," D.C. Flight Approach, No. 32, 1978, pp. 2-7.

[4] Jones, D.M.A. and Sims, A.L., "Climatology of Instantaneous Rainfall Rates," *Journal of Applied Meteorology,* Vol. 17, No. 8, 1978, pp. 1135-1140.

[5] Hershfield, D.M., "Estimating the Extreme-Value 1 Minute Rainfall," *Journal of Applied Meteorology,* Vol. 11, No. 6, 1972, pp. 936-940.

[6] Riordan, P., "Weather Extremes Around the World," Earth Sciences Laboratory, TR-70-45-ES, 1970.

[7] Marshall, J.S. and Palmer, W. McK., "The Distribution of Raindrops With Size," *Journal of Meteorology,* Vol. 5, No. 2, 1948, pp. 165-166.

[8] Merceret, F.J., "Relating Rainfall Rate to the Slope of Raindrop Size Spectra," *Journal of Applied Meterology,* Vol. 14, No. 2, 1975, pp. 259-260.

[9] Markowitz, A.M., "Raindrop Size Distribution Expressions," *Journal of Applied Meteorology,* Vol. 15, No. 9, 1976, pp. 1029-1031.

[10] Haines, P.A. and Luers, J.K., "Aerodynamic Penalties of Heavy Rain on a Landing Aircraft," NASA Contractor Report 156885, July 1982.

[11] Lucey, G.K., "A Rain Impact Analysis for an Artillery PD System," Harry Diamond Laboratories, TM-72-15, May 1972.

[12] Hartley, D.F. and Murgatroyd, W., "Criteria for the Break-up of Thin Liquid Layers Flowing Isothermally over Solid Surface," *International Journal of Heat and Mass Transfer,* Vol. 7, No. 9, 1964, pp. 1002-1015.

[13] Macklin, W.C. and Metaxas, G.J., "Splashing of Drops on Liquid Layers," *Journal of Applied Physics,* Vol. 47, No. 9, 1976, pp. 3963-3970.

[14] Dirling, R.B. Jr., "A Method for Computing Roughwall Heat Transfer Rates on Re-entry Nosetips," Paper 73-763 presented at the AIAA 8th Thermophysics Conference, Palm Springs, Calif., July 16-18, 1973.

[15] Young, F.L., "Experimental Investigation of the Effects of Surface Roughness on Compressible Turbulent Boundary Layer Skin Friction and Heat Transfer," DRL-532, CR-21, May 1965.

[16] Aerodynamic Data for the 747 Aircraft, Boeing Document D6-30643, Vol. II, 1970.

[17] Ljungstroem, B.L.G., "Wind Tunnel Investigation of Simulated Hoar Frost on a 2-Dimensional Wing Section With and Without High Lift Devices," Aeronautical Research Institute of Sweden, Rapport AU-902, 1972.

[18] Kapitza, P.L., "Wave Flow of Thin Layers of a Viscous Fluid," Collected Papers of P.L. Kapitza, New York, 1964, pp. 662-709.

[19] Wurz, D.E., "Experimentelle Untersuchtung des Strömungsverhaltens dünner Wasserfilme und deren Rückwirkung auf einen gleichgerichten Luftstrom mässiger bis hoher Unterschallgeschwindigkeit," Ph.D. thesis, Karlsruhe, Deutschland, 1971.

[20] Wurz, D.E., "Experimental Investigation into the Flow Behaviour of Thin Water Films; Effect on a Concurrent Airflow of Moderate to Heavy Supersonic Velocities. Pressure Distribution at the Surface of Rigid Wary Reference Structures," *Archives of Mechanics,* Vol. 28, No. 5-6, 1976, pp. 969-987.

[21] Luers, J. and Haines, P., "Heavy Rain Influence on Airplane Accidents," *Journal of Aircraft,* Vol. 20, Feb. 1983, pp. 187-191.